# Analysis on the SINR Performance of Dynamic TDD in Homogeneous Small Cell Networks

Ming Ding, National ICT Australia (NICTA), Australia {ming.ding2012@gmail.com}
David López-Pérez, Bell Labs Alcatel-Lucent, Ireland {dr.david.lopez@ieee.org}
Athanasios V. Vasilakos, Kuwait University, Kuwait {th.vasilakos@gmail.com}
Wen Chen, Shanghai Jiao Tong University, China {wenchen@sjtu.edu.cn}

***Abstract*—Small cells are envisioned to embrace dynamic time division duplexing (TDD) in order to tailor downlink (DL)/uplink (UL) subframe resources to the quick variations and burstiness of their DL/UL traffic. In this paper, and for the first time, we perform a theoretical analysis on the signal-to-interference-plus-noise ratio performance of dynamic TDD transmissions in homogeneous small cell networks. The significant accuracy of the proposed theoretical analysis is corroborated by simulations. Based on our work, a partial interference cancellation scheme is proposed to reduce the outage probabilities, and it is shown that cancelling one interfering small cell on average is good enough when the traffic load is low to medium to avoid radio link failures.**

## I. Introduction

Future small cell networks are envisaged to deprecate frequency division duplexing (FDD) schemes and embrace time division duplexing (TDD) schemes, which do not require pairs of spectrum resources [1]. In this line, the 3rd Generation Partnership Project (3GPP) Long Term Evolution (LTE) Release 8-11 networks have already defined seven TDD configurations for semi-static selection at the network side. Each TDD configuration is associated with a downlink (DL)/ uplink (UL) subframe ratio [2]. However, this semi-static selection of TDD configuration is not able to dynamically adapt DL/UL subframe resources to the quick variations in the traffic load of small cells originated due to their low number of connected UEs and the burstiness of their DL/UL traffic.

In order to amend this issue and improve the system capacity in small cell networks, a new technology has been proposed, referred to as dynamic TDD, in which TDD configurations can be dynamically changed in each or a cluster of cells. Dynamic TDD can thus provide a tailored configuration of DL/UL subframe resources at the expense of allowing inter-link interference, i.e., DL-to-UL and UL-to-DL interference. The application of dynamic TDD in homogeneous small cell networks has been investigated in recent works [3], [4]. From simulations, gains in terms of wide-band (WB) signal-to-interference-plus-noise ratio (SINR) and user equipment (UE) packet throughput (UPT) have been observed, mostly in low-to-medium traffic load conditions. However, our understanding of this new technology is still incomplete due to lack of work on its fundamentals.

In this paper and for the first time, we perform a novel theoretical analysis on the SINR performance of dynamic TDD in homogeneous small cell networks. The contribution of this paper is two-fold:

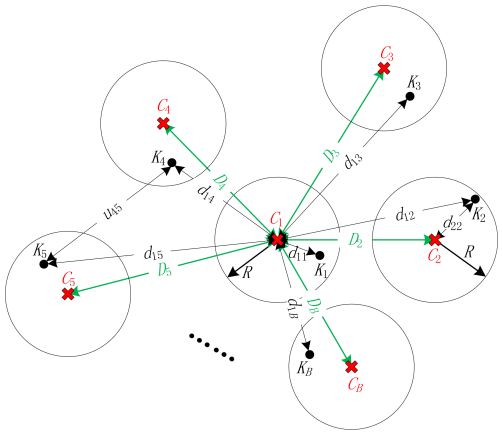


Fig. 1. Schematic model of a homogeneous small cell network.

1) Closed-form expressions for the approximated cumulative density functions (CDFs) of the DL and the UL UE SINRs are derived. Via simulations, the approximated CDFs are verified to be significantly accurate.
2) The developed framework is applied in the design of interference cancellation (IC) schemes for the dynamic TDD UL. A partial IC scheme is proposed to reduce outage probabilities (OPs) using closed-form computations and a standard bisection search.

The rest of the paper is organized as follows: In Section II, the scenario and system model are described. In Section III, our theoretical analysis to derive the UE SINR distribution in a dynamic TDD homogenous small cell network is presented. In Section IV, the application of the developed framework in the design of a partial IC scheme is discussed, and in Section V some concluding remarks are drawn.

## II. Network Scenario

In this paper, we consider a homogeneous small cell network scenario [3], [4], i.e., multiple small cells deployed on the same carrier frequency, as illustrated in Fig. 1.

In Fig. 1, a total of $B$ small cells exist in the network, including one small cell of interest denoted as $C_1$ and $B-1$ interfering small cells denoted as $C_b, b \in \{2, \ldots, B\}$. The radius of the coverage area of each small cell is denoted as $R$. Each small cell base station (BS) is equipped with $N$ antennas.

978-1-4799-3512-3/14/$31.00 ©2014 IEEE

Moreover, it is assumed that in one time-frequency resource, one single-antenna user equipment (UE) is scheduled at each BS to perform a DL or an UL transmission. The UE associated with small cell $C_b$ is denoted as $K_b$, and thus the UE of interest is denoted as $K_1$.

Some UEs $K_b, b \in \{2, \ldots, B\}$ may be de-activated when their instantaneous traffic loads are zero in the DL and the UL. In the following, the modeling of path losses, shadow and multi-path fading, transmit power and small cell activation probability are described.

*The distance* from the BS of $C_b$ to UE $K_m$, $b, m \in \{1, \ldots, B\}$, the distance from UE $K_b$ to UE $K_m$ and the distance from the BS of $C_b$ to the BS of $C_1$ are respectively denoted as $d_{bm}$, $u_{bm}$ and $D_b$.

Based on $d_{bm}$, $u_{bm}$ and $D_b$, *the path loss* from the BS of $C_b$ to UE $K_m$, the path loss from UE $K_b$ to UE $K_m$ and the path loss from the BS of $C_b$ to the BS of $C_1$ are respectively modeled as

$$PL_{bm}^{\mathrm{BS2UE}} = A_1 + \alpha_1 \log_{10} d_{bm}, \quad (1)$$

$$PL_{bm}^{\mathrm{UE2UE}} = A_2 + \alpha_2 \log_{10} u_{bm}, \quad (2)$$

$$PL_{b}^{\mathrm{BS2BS}} = A_3 + \alpha_3 \log_{10} D_b, \quad (3)$$

where $A_i$ and $\alpha_i$, $i \in \{1, 2, 3\}$ are constants obtained from field tests [1]. Path losses are in dB and distances in km.

It is important to note that for a certain $i$, $A_i$ and $\alpha_i$ may take different values for the line-of-sight (LoS) transmission case and the non-LoS (NLoS) transmission case. Besides, the LoS probability is normally a monotonically decreasing function with respect to the distance $dis$ in km between the transmitter and the receiver. For example, in [1], the LoS probability function is modeled as

$$\begin{aligned} \Pr^{\mathrm{LoS}}(dis) &= 0.5 - \min\{0.5, 5\exp(-0.156/dis)\} \\ &\quad + \min\{0.5, 5\exp(-1 \times dis/0.03)\}. \end{aligned} \quad (4)$$

*The shadow fading* from the BS of $C_b$ to UE $K_m$, the shadow fading from UE $K_b$ to UE $K_m$ and the shadow fading from the BS of $C_b$ to the BS of $C_1$ are respectively denoted as $S_{bm}^{\mathrm{BS2UE}}$, $S_{bm}^{\mathrm{UE2UE}}$ and $S_{b}^{\mathrm{BS2BS}}$. The dB-scale shadow fading is usually modeled as a normal random variable (RV), and it is not an independent variable. In [1], it is suggested that the standard deviation (STD) of $S_{bm}^{\mathrm{BS2UE}}$ should be 10 dB and the correlation coefficient between $S_{bm}^{\mathrm{BS2UE}}$ and $S_{lm}^{\mathrm{BS2UE}}$ $(b \neq l)$ should be 0.5.

Taking into account path loss and shadowing, for the convenience of mathematical expression in the sequel, the following auxiliary variables are defined

$$\gamma_{bm}^{\mathrm{BS2UE}} = 10^{-\frac{PL_{bm}^{\mathrm{BS2UE}} + S_{bm}^{\mathrm{BS2UE}}}{10}} \Big/ N_0,$$

$$\gamma_{bm}^{\mathrm{UE2UE}} = 10^{-\frac{PL_{bm}^{\mathrm{UE2UE}} + S_{bm}^{\mathrm{UE2UE}}}{10}} \Big/ N_0,$$

$$\gamma_{b}^{\mathrm{BS2BS}} = 10^{-\frac{PL_{b}^{\mathrm{BS2BS}} + S_{b}^{\mathrm{BS2BS}}}{10}} \Big/ N_0,$$

where $N_0$ is the additive white Gaussian noise (AWGN) power.

*The multi-path fading* channel from the BS of $C_b$ to UE $K_m$, the multi-path fading channel from UE $K_b$ to UE $K_m$ and the multi-path fading channel from the BS of $C_b$ to the BS of $C_1$ are respectively denoted as $\mathbf{h}_{bm}^{\mathrm{BS2UE}} \in \mathbb{C}^{1\times N}$, $\mathbf{h}_{bm}^{\mathrm{UE2UE}} \in \mathbb{C}$ and $\mathbf{H}_{b}^{\mathrm{BS2BS}} \in \mathbb{C}^{N\times N}$. All channels are assumed to experience uncorrelated flat Rayleigh fading on the considered time-frequency resource, and the channel coefficients are modeled as independently identical distributed (i.i.d.) zero-mean circularly symmetric complex Gaussian (ZMCSCG) RVs with unit variance.

*The transmit power* of the BS of small cell $C_b$ and the transmit power of UE $K_b$ are respectively denoted as $P_b^{\mathrm{BS}}$ and $P_b^{\mathrm{UE}}$. In practice, $P_b^{\mathrm{BS}}$ is usually a cell-specific constant to maintain a stable DL coverage, while $P_b^{\mathrm{UE}}$ is subject to semi-static power control (PC) such as the fractional path loss compensation (FPC) scheme [2]. In more detail, the FPC scheme is modeled as

$$P_b^{\mathrm{UE}} = 10^{\frac{1}{10}\left(P_0 + \eta\left(PL_{bb}^{\mathrm{BS2UE}} + S_{bb}^{\mathrm{BS2UE}}\right) + 10\log_{10} N_{\mathrm{RB}}\right)}, \quad (5)$$

where $P_0$ is the power basis in dBm, $\eta$ is the FPC factor and $N_{\mathrm{RB}}$ is the number of resource blocks (RBs) in use by the UE. Each RB spans across 180 KHz in the 3GPP LTE networks [2].

Finally, *the activation probability* of each interfering small cell is assumed to be $\rho_0$, which reflects the traffic load condition in the network. When an interfering small cell is activated, the probabilities of such small cell transmiting in DL or UL are respectively denoted as $\rho^{\mathrm{DL}}$ and $\rho^{\mathrm{UL}}$, with $\rho^{\mathrm{DL}} + \rho^{\mathrm{UL}} = 1$.

## III. Analytical SINR Results in Dynamic TDD

We suppose that small cells $C_b, b \in \Psi^{\mathrm{DL}}$ and $C_b, b \in \Psi^{\mathrm{UL}}$ conduct DL and UL transmissions, respectively. Here, we assume $\Psi^{\mathrm{DL}} \cup \Psi^{\mathrm{UL}} \neq \emptyset$ and we further denote $\Psi^{\mathrm{M}}$ as the index set of small cells that are muted due to no traffic. It is evident that $\Psi^{\mathrm{DL}} \cup \Psi^{\mathrm{UL}} \cup \Psi^{\mathrm{M}} = \{2, \ldots, B\}$, and that the intersection of any two sets from $\Psi^{\mathrm{DL}}$, $\Psi^{\mathrm{UL}}$ and $\Psi^{\mathrm{M}}$ is an empty set.

Let us now consider the UE of interest, i.e., $K_1$ in small cell $C_1$. Its received signal in the DL and the UL when dynamic TDD is engaged can be respectively modeled as

$$\begin{aligned} & r_1^{\mathrm{DL}}\left(\Psi^{\mathrm{DL}}, \Psi^{\mathrm{UL}}\right) \\ &= \sqrt{\gamma_{11}^{\mathrm{BS2UE}} N_0}\, \mathbf{h}_{11}^{\mathrm{BS2UE}} \sqrt{P_b^{\mathrm{BS}}}\, \mathbf{w}_1 v_1 \\ &\quad + \sum_{b\in\Psi^{\mathrm{DL}}} \sqrt{\gamma_{b1}^{\mathrm{BS2UE}} N_0}\, \mathbf{h}_{b1}^{\mathrm{BS2UE}} \sqrt{P_b^{\mathrm{BS}}}\, \mathbf{w}_b v_b \\ &\quad + \sum_{b\in\Psi^{\mathrm{UL}}} \sqrt{\gamma_{b1}^{\mathrm{UE2UE}} N_0}\, \mathbf{h}_{b1}^{\mathrm{UE2UE}} \sqrt{P_b^{\mathrm{UE}}}\, v_b + n_1^{\mathrm{DL}}, \end{aligned} \quad (6)$$

and

$$\begin{aligned} & r_1^{\mathrm{UL}}\left(\Psi^{\mathrm{DL}}, \Psi^{\mathrm{UL}}\right) \\ &= \mathbf{f}_1\Big(\sqrt{\gamma_{11}^{\mathrm{BS2UE}} N_0}\left(\mathbf{h}_{11}^{\mathrm{BS2UE}}\right)^{\mathrm{H}} \sqrt{P_1^{\mathrm{UE}}} v_1 \\ &\quad + \sum_{b\in\Psi^{\mathrm{DL}}} \sqrt{\gamma_{b}^{\mathrm{BS2BS}} N_0}\, \mathbf{H}_{b}^{\mathrm{BS2BS}} \sqrt{P_b^{\mathrm{BS}}}\, \mathbf{w}_b v_b \\ &\quad + \sum_{b\in\Psi^{\mathrm{UL}}} \sqrt{\gamma_{1b}^{\mathrm{BS2UE}} N_0}\left(\mathbf{h}_{1b}^{\mathrm{BS2UE}}\right)^{\mathrm{H}} \sqrt{P_b^{\mathrm{UE}}} v_b + \mathbf{n}_1^{\mathrm{UL}}\Big), \end{aligned} \quad (7)$$

where $v_b$ is the data symbol of UE $K_b$, $\mathbf{w}_b \in \mathbb{C}^{N\times 1}$ is the DL precoder used by the BS of small cell $C_b$ for UE $K_b$, $\mathbf{f}_1 \in \mathbb{C}^{1\times N}$ is the UL receiving filter at small cell $C_1$, $n_1^{\mathrm{DL}}$ is the ZMCSCG noise value in the DL at UE $K_1$, and $\mathbf{n}_1^{\mathrm{UL}}$ is the ZMCSCG noise vector in the UL at the BS of small cell $C_1$. Without loss of generality, we assume that $v_b$, $\mathbf{w}_b$, $\mathbf{f}_1$, $n_1^{\mathrm{DL}}$ and $\mathbf{n}_1^{\mathrm{UL}}$ respectively satisfy $\mathrm{E}\left\{v_b v_b^{\mathrm{H}}\right\} = 1$, $\mathrm{Tr}\left\{\mathbf{w}_b\mathbf{w}_b^{\mathrm{H}}\right\} = 1$, $\mathrm{Tr}\left\{\mathbf{f}_1\mathbf{f}_1^{\mathrm{H}}\right\} = 1$, $\mathrm{E}\left\{n_1^{\mathrm{DL}}\left(n_1^{\mathrm{DL}}\right)^{\mathrm{H}}\right\} = N_0$ and $\mathrm{E}\left\{\mathbf{n}_1^{\mathrm{UL}}\left(\mathbf{n}_1^{\mathrm{UL}}\right)^{\mathrm{H}}\right\} = N_0\mathbf{I}$.

From (6) and (7), the DL and the UL SINRs of UE $K_1$ as a function of $\left(\Psi^{\mathrm{DL}}, \Psi^{\mathrm{UL}}\right)$ can be respectively derived as (8) and (9), which are shown on the top of next page. In (8) and (9), $\gamma_{b1}^{\mathrm{BS2UE}}P_b^{\mathrm{BS}}$ and $\gamma_{b1}^{\mathrm{UE2UE}}P_b^{\mathrm{UE}}$, as well as $\gamma_b^{\mathrm{BS2BS}}P_b^{\mathrm{BS}}$ and $\gamma_{1b}^{\mathrm{BS2UE}}P_b^{\mathrm{UE}}$ are received WB signal-to-noise ratios (SNR) at UE/BS, which can be known from measurement reports associated with DL/UL reference signals (RSs). Due to the relatively slow variation of WB SNRs in practical wireless channels, such information is assumed to be perfectly known in this paper. And hence, in the following, we will focus on the analysis of the DL and the UL SINR of UE $K_1$ with respect to the RVs originated due to multi-path fading. As the first step of theoretical analysis, we assume that perfect information of multi-path fading is available at transmitters.

### A. DL SINR with RVs of Multi-Path Fading

In the DL, we consider the non-cooperative normalized maximal ratio transmission (MRT) for small cell BSs, i.e., $\mathbf{w}_b = \frac{\left(\mathbf{h}_{bb}^{\mathrm{BS2UE}}\right)^{\mathrm{H}}}{\left\|\mathbf{h}_{bb}^{\mathrm{BS2UE}}\right\|}$. With some mathematical manipulation, the conditional RV $Z_1^{\mathrm{DL}}\left(\Psi^{\mathrm{DL}}, \Psi^{\mathrm{UL}}\right)$ can be reformulated as

$$Z_1^{\mathrm{DL}}\left(\Psi^{\mathrm{DL}}, \Psi^{\mathrm{UL}}\right) = \frac{\gamma_{11}^{\mathrm{BS2UE}}P_1^{\mathrm{BS}}X_1^{\mathrm{DL}}}{\sum\limits_{b\in\Psi^{\mathrm{DL}}}\gamma_{b1}^{\mathrm{BS2UE}}P_b^{\mathrm{BS}}Y_{b1}^{\mathrm{DL2DL}} + \sum\limits_{b\in\Psi^{\mathrm{UL}}}\gamma_{b1}^{\mathrm{UE2UE}}P_b^{\mathrm{UE}}Y_{b1}^{\mathrm{UL2DL}} + 1}, \tag{10}$$

where

$$\begin{aligned} X_1^{\mathrm{DL}} &= \left|\mathbf{h}_{11}^{\mathrm{BS2UE}}\mathbf{w}_1\right|^2 \\ &= \left|\mathbf{h}_{11}^{\mathrm{BS2UE}}\frac{\left(\mathbf{h}_{11}^{\mathrm{BS2UE}}\right)^{\mathrm{H}}}{\left\|\mathbf{h}_{11}^{\mathrm{BS2UE}}\right\|}\right|^2 \\ &= \left\|\mathbf{h}_{11}^{\mathrm{BS2UE}}\right\|^2, \end{aligned} \tag{11}$$

$$\begin{aligned} Y_{b1}^{\mathrm{DL2DL}} &= \left|\mathbf{h}_{b1}^{\mathrm{BS2UE}}\mathbf{w}_b\right|^2 \\ &= \left|\mathbf{h}_{b1}^{\mathrm{BS2UE}}\frac{\left(\mathbf{h}_{bb}^{\mathrm{BS2UE}}\right)^{\mathrm{H}}}{\left\|\left(\mathbf{h}_{bb}^{\mathrm{BS2UE}}\right)^{\mathrm{H}}\right\|}\right|^2, \end{aligned} \tag{12}$$

$$Y_{b1}^{\mathrm{UL2DL}} = \left|\mathbf{h}_{b1}^{\mathrm{UE2UE}}\right|^2. \tag{13}$$

According to [5], $X_1^{\mathrm{DL}}$ and $Y_{b1}^{\mathrm{UL2DL}}$ follow chi-squared distributions with $2N$ and 2 degrees of freedom, respectively. Regarding $Y_{b1}^{\mathrm{DL2DL}}$, for a given $\mathbf{w}_b$, $\mathbf{h}_{b1}^{\mathrm{BS2UE}}\mathbf{w}_b$ can be deemed as a weighted sum of $N$ i.i.d. Rayleigh fading coefficients, which leads to a new Rayleigh fading coefficient, because the norm of $\mathbf{w}_b$ is one and the phases of the elements in $\mathbf{h}_{b1}^{\mathrm{BS2UE}}$ and $\mathbf{w}_b$ are random and uncorrelated. Since such distribution does not vary with $\mathbf{w}_b$, we can conclude that $Y_{b1}^{\mathrm{DL2DL}}$ also follows a chi-squared distribution with 2 degrees of freedom.

### B. UL SINR with RVs of Multi-Path Fading

In the UL, we consider a normalized maximal ratio combining (MRC) filter, which is expressed as $\mathbf{f}_1 = \frac{\mathbf{h}_{11}^{\mathrm{BS2UE}}}{\left\|\mathbf{h}_{11}^{\mathrm{BS2UE}}\right\|}$. With some mathematical manipulation, the conditional RV $Z_1^{\mathrm{UL}}\left(\Psi^{\mathrm{DL}}, \Psi^{\mathrm{UL}}\right)$ can be rewritten as

$$Z_1^{\mathrm{UL}}\left(\Psi^{\mathrm{DL}}, \Psi^{\mathrm{UL}}\right) = \frac{\gamma_{11}^{\mathrm{BS2UE}}P_1^{\mathrm{UE}}X_1^{\mathrm{UL}}}{\sum\limits_{b\in\Psi^{\mathrm{DL}}}\gamma_b^{\mathrm{BS2BS}}P_b^{\mathrm{BS}}Y_{b1}^{\mathrm{DL2UL}} + \sum\limits_{b\in\Psi^{\mathrm{UL}}}\gamma_{1b}^{\mathrm{BS2UE}}P_b^{\mathrm{UE}}Y_{b1}^{\mathrm{UL2UL}} + 1}, \tag{14}$$

where

$$\begin{aligned} X_1^{\mathrm{UL}} &= \left|\mathbf{f}_1\left(\mathbf{h}_{11}^{\mathrm{BS2UE}}\right)^{\mathrm{H}}\right|^2 \\ &= \left|\frac{\mathbf{h}_{11}^{\mathrm{BS2UE}}}{\left\|\mathbf{h}_{11}^{\mathrm{BS2UE}}\right\|}\left(\mathbf{h}_{11}^{\mathrm{BS2UE}}\right)^{\mathrm{H}}\right|^2 \\ &= \left\|\mathbf{h}_{11}^{\mathrm{BS2UE}}\right\|^2, \end{aligned} \tag{15}$$

$$\begin{aligned} Y_{b1}^{\mathrm{DL2UL}} &= \left|\mathbf{f}_1\mathbf{H}_b^{\mathrm{BS2BS}}\mathbf{w}_b\right|^2 \\ &= \left|\frac{\mathbf{h}_{11}^{\mathrm{BS2UE}}}{\left\|\mathbf{h}_{11}^{\mathrm{BS2UE}}\right\|}\mathbf{H}_b^{\mathrm{BS2BS}}\frac{\left(\mathbf{h}_{bb}^{\mathrm{BS2UE}}\right)^{\mathrm{H}}}{\left\|\mathbf{h}_{bb}^{\mathrm{BS2UE}}\right\|}\right|^2, \end{aligned} \tag{16}$$

$$\begin{aligned} Y_{b1}^{\mathrm{UL2UL}} &= \left|\mathbf{f}_1\left(\mathbf{h}_{1b}^{\mathrm{BS2UE}}\right)^{\mathrm{H}}\right|^2 \\ &= \left|\frac{\mathbf{h}_{11}^{\mathrm{BS2UE}}}{\left\|\mathbf{h}_{11}^{\mathrm{BS2UE}}\right\|}\left(\mathbf{h}_{1b}^{\mathrm{BS2UE}}\right)^{\mathrm{H}}\right|^2. \end{aligned} \tag{17}$$

According to [5], $X_1^{\mathrm{UL}}$ follows a chi-squared distribution with $2N$ degrees of freedom. In addition, similar to $Y_{b1}^{\mathrm{DL2DL}}$, $Y_{b1}^{\mathrm{UL2UL}}$ also follows a chi-squared distribution with 2 degrees of freedom. As for $Y_{b1}^{\mathrm{DL2UL}}$, we obtain its distribution using the following Lemma.

**Lemma 1.** *$Y_{b1}^{\mathrm{DL2UL}}$ follows a chi-squared distribution with 2 degrees of freedom.*

*Proof:* See Appendix I. ∎

### C. CDF of the DL/UL SINR

Taking into account the equivalences in (18) and (19) shown on the top of next page, we transform (10) and (14) into

$$Z = \frac{\beta X}{\sum\limits_{b=1}^{\tilde{B}}\mu_b Y_b + 1}, \tag{20}$$

where the sum of cardinalities of $\Psi^{\mathrm{DL}}$ and $\Psi^{\mathrm{UL}}$ is denoted as $\tilde{B}$, i.e., $\tilde{B} = \mathrm{Card}\left\{\Psi^{\mathrm{DL}}\right\} + \mathrm{Card}\left\{\Psi^{\mathrm{UL}}\right\}$, where $\mathrm{Card}\{\Psi\}$ retrieves the cardinality of a set $\Psi$ and $\mathrm{Card}\{\emptyset\} = 0$. It is obvious that $\tilde{B} \le B - 1$.

Considering (20), it is worth recalling that:

- $X$ follows a chi-squared distribution with $2N$ degrees of freedom and its CDF is [5]

$$Z_1^{\mathrm{DL}}\left(\Psi^{\mathrm{DL}},\Psi^{\mathrm{UL}}\right)=\frac{\gamma_{11}^{\mathrm{BS2UE}}P_1^{\mathrm{BS}}\left|\mathbf{h}_{11}^{\mathrm{BS2UE}}\mathbf{w}_1\right|^2}{\sum\limits_{b\in\Psi^{\mathrm{DL}}}\gamma_{b1}^{\mathrm{BS2UE}}P_b^{\mathrm{BS}}\left|\mathbf{h}_{b1}^{\mathrm{BS2UE}}\mathbf{w}_b\right|^2+\sum\limits_{b\in\Psi^{\mathrm{UL}}}\gamma_{b1}^{\mathrm{UE2UE}}P_b^{\mathrm{UE}}\left|\mathbf{h}_{b1}^{\mathrm{UE2UE}}\right|^2+1}. \tag{8}$$

$$Z_1^{\mathrm{UL}}\left(\Psi^{\mathrm{DL}},\Psi^{\mathrm{UL}}\right)=\frac{\gamma_{11}^{\mathrm{BS2UE}}P_1^{\mathrm{UE}}\left|\mathbf{f}_1\left(\mathbf{h}_{11}^{\mathrm{BS2UE}}\right)^{\mathrm{H}}\right|^2}{\sum\limits_{b\in\Psi^{\mathrm{DL}}}\gamma_b^{\mathrm{BS2BS}}P_b^{\mathrm{BS}}\left|\mathbf{f}_1\mathbf{H}_b^{\mathrm{BS2BS}}\mathbf{w}_b\right|^2+\sum\limits_{b\in\Psi^{\mathrm{UL}}}\gamma_{1b}^{\mathrm{BS2UE}}P_b^{\mathrm{UE}}\left|\mathbf{f}_1\left(\mathbf{h}_{1b}^{\mathrm{BS2UE}}\right)^{\mathrm{H}}\right|^2+1}. \tag{9}$$

$$Z\left(\begin{array}{l}\beta=\gamma_{11}^{\mathrm{BS2UE}}P_1^{\mathrm{BS}}\\ \mu_b=\left\{\left\{\gamma_{b1}^{\mathrm{BS2UE}}P_b^{\mathrm{BS}}\middle|\, b\in\Psi^{\mathrm{DL}}\right\},\left\{\gamma_{b1}^{\mathrm{UE2UE}}P_b^{\mathrm{UE}}\middle|\, b\in\Psi^{\mathrm{UL}}\right\}\right\}\end{array}\right)=Z_1^{\mathrm{DL}}\left(\Psi^{\mathrm{DL}},\Psi^{\mathrm{UL}}\right). \tag{18}$$

$$Z\left(\begin{array}{l}\beta=\gamma_{11}^{\mathrm{BS2UE}}P_1^{\mathrm{UE}}\\ \mu_b=\left\{\left\{\gamma_b^{\mathrm{BS2BS}}P_b^{\mathrm{BS}}\middle|\, b\in\Psi^{\mathrm{DL}}\right\},\left\{\gamma_{1b}^{\mathrm{BS2UE}}P_b^{\mathrm{UE}}\middle|\, b\in\Psi^{\mathrm{UL}}\right\}\right\}\end{array}\right)=Z_1^{\mathrm{UL}}\left(\Psi^{\mathrm{DL}},\Psi^{\mathrm{UL}}\right). \tag{19}$$

$$P_X(x)=1-\mathrm{e}^{-x}\sum_{l=0}^{N-1}\frac{x^l}{l!}. \tag{21}$$

- $Y_b$s are i.i.d. chi-squared RVs with 2 degrees of freedom.

Now, let us focus on the denominator of (20), and investigate the distribution of a RV $Y^{\mathrm{sum}}$ defined as $Y^{\mathrm{sum}}=\sum\limits_{b=1}^{\tilde{B}}\mu_bY_b$. In [6], the authors proposed that the distribution of a weighted sum of squared normal RVs can be well approximated by a gamma distribution. In more detail, let $G_b, b\in\{1,2,\ldots,L\}$ be $L$ i.i.d. normal RVs with zero mean and unit variance, and $G^{\mathrm{sum}}=\sum\limits_{b=1}^{L}a_bG_b^2$, where $a_b\in\mathbb{R}^+$. Then, the CDF of $G^{\mathrm{sum}}$ can be approximated by an incomplete gamma function written as $P_{G^{\mathrm{sum}}}(g)\approx\int_0^g\frac{\omega^\lambda}{\Gamma(\lambda)}\exp(-\omega t)\,t^{\lambda-1}dt$, where $\omega=\sum\limits_{b=1}^{L}a_b/2\sum\limits_{b=1}^{L}a_b^2$ and $\lambda=\left(\sum\limits_{b=1}^{L}a_b\right)^2/2\sum\limits_{b=1}^{L}a_b^2$. Following this recipe and since in (20) each $Y_b$ is a sum of two i.i.d. squared normal RVs $Y_{b1}$ and $Y_{b2}$, the CDF of $Y^{\mathrm{sum}}=\sum\limits_{b=1}^{\tilde{B}}\mu_bY_b=\sum\limits_{b=1}^{\tilde{B}}\mu_bY_{b1}+\sum\limits_{b=1}^{\tilde{B}}\mu_bY_{b2}$ can be approximately modeled as

$$P_{Y^{\mathrm{sum}}}(y)\approx\int_0^y\frac{\omega^\lambda}{\Gamma(\lambda)}\exp(-\omega t)\,t^{\lambda-1}dt, \tag{22}$$

where $\omega=\dfrac{\sum\limits_{b=1}^{\tilde{B}}2\mu_b}{2\sum\limits_{b=1}^{\tilde{B}}2\mu_b^2}$ and $\lambda=\dfrac{\left(\sum\limits_{b=1}^{\tilde{B}}2\mu_b\right)^2}{2\sum\limits_{b=1}^{\tilde{B}}2\mu_b^2}$ are computed according to (18) for the DL or (19) for the UL. From (22), the probability density function (PDF) of $Y^{\mathrm{sum}}$ can be approximately modeled as

$$p_{Y^{\mathrm{sum}}}(y)\approx\frac{\omega^\lambda}{\Gamma(\lambda)}\exp(-\omega y)\,y^{\lambda-1}. \tag{23}$$

Note that this gamma approximation is remarkably accurate and we refer interested readers to [6] for more details.

Based on the previous definition, we claim in this paper that the CDF of $Z$ can be found using Theorem 2.

**Theorem 2.** *The CDF of $Z$ can be approximated as*

$$P_Z(z)\approx Q(\omega,\lambda,\beta,z), \tag{24}$$

where $Q(\omega,\lambda,\beta,z)$

$=1-\frac{\omega^\lambda}{\Gamma(\lambda)}\exp\left(-\frac{z}{\beta}\right)\sum\limits_{l=0}^{N-1}\sum\limits_{k=0}^{l}\frac{\Gamma(k+\lambda)}{k!(l-k)!}\left(\frac{z}{\beta}\right)^l\left(\frac{\beta}{z+\omega\beta}\right)^{k+\lambda}$.

*Proof:* See Appendix II. ■

When all interfering BSs are muted, (20) will degenerate to a trivial RV as

$$Z=\beta X, \tag{25}$$

and its CDF can be easily obtained from (21) as

$$\begin{aligned}P_Z(z)&=\Pr\left(X\le\frac{z}{\beta}\right)\\&=1-\exp\left(-\frac{z}{\beta}\right)\sum_{l=0}^{N-1}\frac{1}{l!}\left(\frac{z}{\beta}\right)^l\\&\triangleq F(\beta,z).\end{aligned} \tag{26}$$

Then, the CDFs of $Z_1^{\mathrm{DL}}\left(\Psi^{\mathrm{DL}}=\Psi^{\mathrm{UL}}=\emptyset\right)$ and $Z_1^{\mathrm{UL}}\left(\Psi^{\mathrm{DL}}=\Psi^{\mathrm{UL}}=\emptyset\right)$ can be readily obtained from (26) using the following equivalence between variables,

$$Z\left(\beta=\gamma_{11}^{\mathrm{BS2UE}}P_1^{\mathrm{BS}}\right)=Z_1^{\mathrm{DL}}\left(\Psi^{\mathrm{DL}}=\Psi^{\mathrm{UL}}=\emptyset\right), \tag{27}$$

and

$$Z\left(\beta=\gamma_{11}^{\mathrm{BS2UE}}P_1^{\mathrm{UE}}\right)=Z_1^{\mathrm{UL}}\left(\Psi^{\mathrm{DL}}=\Psi^{\mathrm{UL}}=\emptyset\right). \tag{28}$$

Taking this particular case into consideration, the CDF of $Z_1^{\mathrm{DL}}(Z_1^{\mathrm{UL}})$ for any number of interfering cells can be derived from (24) and (26) with the enumeration over all the possible combinations of $\Psi^{\mathrm{DL}}$, $\Psi^{\mathrm{UL}}$ and $\Psi^{\mathrm{M}}$. The probability of each combination $\left(\Psi^{\mathrm{DL}},\Psi^{\mathrm{UL}},\Psi^{\mathrm{M}}\right)$ can be calculated as

$$\begin{aligned}&\rho\left(\Psi^{\mathrm{M}},\Psi^{\mathrm{DL}},\Psi^{\mathrm{UL}}\right)\\&=(1-\rho_0)^{\mathrm{Card}\left\{\Psi^{\mathrm{M}}\right\}}\left(\rho_0\rho^{\mathrm{DL}}\right)^{\mathrm{Card}\left\{\Psi^{\mathrm{DL}}\right\}}\left(\rho_0\rho^{\mathrm{UL}}\right)^{\mathrm{Card}\left\{\Psi^{\mathrm{UL}}\right\}}.\end{aligned} \tag{29}$$

Note that the probability of all interfering small cells being muted is $(1-\rho_0)^{B-1}$. Therefore, the CDF of $Z_1^{\mathrm{DL}}$ and $Z_1^{\mathrm{UL}}$ can be modeled as

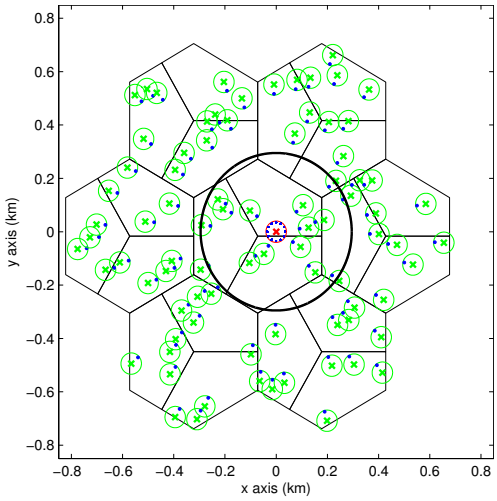


Fig. 2. Illustration of the considered 3GPP network scenario.

$$P_{Z_1}(z) = \sum_{\substack{\Psi^{\mathrm{M}},\Psi^{\mathrm{DL}},\Psi^{\mathrm{UL}} \\ \Psi^{\mathrm{DL}} \bigcup \Psi^{\mathrm{UL}} \neq \emptyset}} \rho\left(\Psi^{\mathrm{M}},\Psi^{\mathrm{DL}},\Psi^{\mathrm{UL}}\right) Q(\omega,\lambda,\beta,z_1) + (1-\rho_0)^{B-1} F(\beta,z_1). \quad (30)$$

For the DL, $Z_1$, $z_1$ in $Q(\omega,\lambda,\beta,z_1)$ and $z_1$ in $F(\beta,z_1)$ should be replaced by $Z_1^{\mathrm{DL}}$, $z$ in (18), and $z$ in (27), respectively. For the UL, $Z_1$, $z_1$ in $Q(\omega,\lambda,\beta,z_1)$ and $z_1$ in $F(\beta,z_1)$ should be replaced by $Z_1^{\mathrm{UL}}$, $z$ in (19), and $z$ in (28), respectively.

## IV. Validation of the Developed Framework

In this section, we discuss the importance of parameter $B$ (the number of small cells in the analysis), and verify the correctness of the analytical results shown by (30) through simulations. Here, we consider a practical homogeneous small cell network scenario adopted by the 3GPP [7]. Fig. 2 shows a snapshot of the considered scenario, and Table I presents its key parameters. Note that according to 3GPP recommendation [1], the DL-to-UL ratio of traffic loads is assumed to be 2:1, and thus in our simulation the ratio of $\rho^{\mathrm{DL}}$ to $\rho^{\mathrm{UL}}$ is also set to 2:1. In Fig. 2, the red circle and the red x-marker represent $C_1$ and its associated BS, respectively. Surrounding $C_1$ there are 83 interfering small cells/BSs represented by green circles/x-markers. In order to consider a worst case scenario, we assume that UE $K_1$ is located at the cell edge of $C_1$ with $d_{11} = 0.035$ km, which is near the fringe of the 40-meter-radius coverage of $C_1$. Furthermore, all interfering UEs are placed on the segments between the BS of $C_1$ and those of $C_b$s with $d_{bb} = 0.035$ km. Fig. 2 shows the possible position of UE $K_1$ plotted as a dotted blue circle and the interfering UEs plotted as blue dots.

### A. The Appropriate Value of $B$

It is computationally difficult to obtain the analytical or numerical results of the DL/UL SINR CDF of UE $K_1$ if all the 83 interferers should be taken into account. Fortunately, a large number of interfering small cells can be ignored [8] if their interference signal strengths are significantly lower than

Table I
Key Parameters of the Considered Network Scenario [1]

| Parameters | Assumptions |
|---|---|
| Scenario | Multiple small cells, co-channel deploy. |
| Cellular model | 7 dummy macrocell sites<br>3 macrocells in each site<br>wrap-around |
| Inter-site distance | 500 m |
| Picocell deployment | 4 picocells per macrocell<br>40 m radius<br>random deployment |
| System band width (BW) | 1.08 MHz (6 RBs) |
| Min. Pico-to-Pico distance | 40 m |
| Min. UE-to-Pico distance | 10 m |
| Antenna number (picocell) | 4 for both Tx and Rx |
| Antenna number (UE) | 1 for both Tx and Rx |
| $P_b^{\mathrm{BS}}$ | 7 dBm (scaled from 24 dBm for 10 MHz) |
| Parameters to obtain $P_b^{\mathrm{UE}}$ | $P_0 = -76$ dBm, $\eta = 0.8$, $N_{\mathrm{RB}} = 6$ |
| $N_0$ | -113.7 dBm (computed from -174 dBm/Hz) |
| BS-to-UE path loss | LoS: $A_1 = 103.8, \alpha_1 = 20.9$<br>NLoS: $A_1 = 145.4, \alpha_1 = 37.5$<br>The probability of LoS: see (4) |
| UE-to-UE path loss | LoS ($u_{bm} \leq 50$ m): $A_2 = 98.45, \alpha_2 = 20$<br>NLoS ($u_{bm} > 50$ m): $A_2 = 175.78, \alpha_2 = 40$ |
| BS-to-BS path loss | LoS: $A_3 = 98.4, \alpha_3 = 20$<br>NLoS: $A_3 = 169.36, \alpha_3 = 40$<br>The probability of LoS: see (4) |
| STD of $S_{bm}^{\mathrm{BS2UE}}$ | 10 dB |
| STD of $S_{bm}^{\mathrm{UE2UE}}$ | 12 dB |
| STD of $S_b^{\mathrm{BS2BS}}$ | 6 dB |
| Shadow correlation | 0 (between UEs), 0.5 (between Picos) |
| $\rho_0$ | 0.3 (low-to-medium traffic load condition) |
| $\rho^{\mathrm{DL}}$,$\rho^{\mathrm{UL}}$ | 2/3, 1/3 |

that arriving at the BS of $C_1$ in the UL or at UE $K_1$ in the DL. From Table I, we can find that NLoS is assumed for UE-to-UE links due to the low heights of UEs, and that the UE-to-UE path loss is generally larger than the BS-to-UE and the BS-to-BS ones when the UE-to-UE distance is large than 50 m. In contrast, the presence of LoS has a significant impact on the BS-to-UE and the BS-to-BS path losses. To be more specific, compared with the BS-to-UE path loss with LoS, the BS-to-UE path loss with NLoS suffers from an additional attenuation that is more than 40 dB, as well as a nearly double loss with regard to $d_{bm}$. Compared with the BS-to-BS path loss with LoS, the BS-to-BS path loss with NLoS is severely penalized by about 70 dB on top of the double loss. Hence, we assume that a small cell $C_b$ can be dismissed from our analysis when the probability of LoS from its BS to any UE as well as the BS in $C_1$ is lower than a predefined threshold $\tau$, i.e.,

$$\Pr^{\mathrm{LoS}}(D_b - R) < \tau, \quad (31)$$

where (31) is BS-oriented because interference originated from a UE is typically much smaller than that from a BS due to the lower transmission power of a UE. In our analysis, $\tau$= 0.001 so that only minor interfering small cells are taken out of the picture. The minimum $D_b$ that satisfies (31) can obtained from a standard bisection search process [9]. Based on (4) and (31), small cells with $D_b > 0.3138$ km are ignored in our analysis. The simplified network by removing small cells satisfying (31) is enclosed by a black circle in Fig. 2, where a small cell is ignored if its associated BS is located outside the black circle.

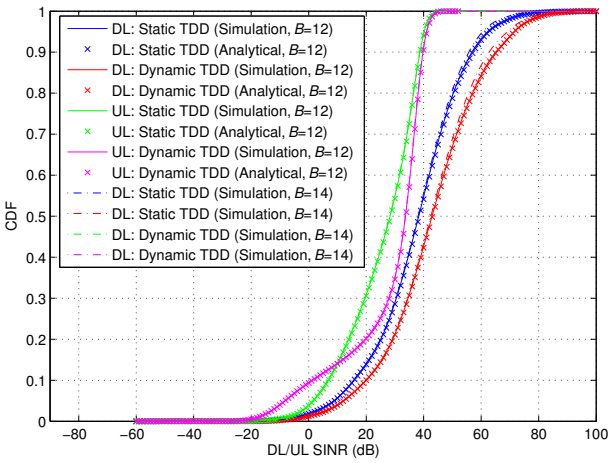


Fig. 3. CDFs of the DL and the UL SINRs for a cell-edge UE.

According to this new scenario depicted by Fig. 2, the value of $B$ is set to 12 for the computation of (30).

### *B. Verification of Our Analytical Results*

Based on the parameters listed in Table I, we perform 100 independent drops in the network scenario illustrated by Fig. 2. For each drop, $\gamma_{bm}^{\mathrm{BS2UE}}$, $\gamma_{bm}^{\mathrm{UE2UE}}$ and $\gamma_{b}^{\mathrm{BS2BS}}$ are randomly regenerated, and UE $K_1$ is randomly placed at a point on the blue dotted circle in Fig. 2. Moreover, in each drop, all channels are modeled as i.i.d. Rayleigh fading and 1,000 experiments are conducted for each combination of $\left(\Psi^{\mathrm{DL}}, \Psi^{\mathrm{UL}}, \Psi^{\mathrm{M}}\right)$ to obtain the numerical results. Fig. 3 shows the average CDFs of the DL and the UL SINRs. As can be seen from it, our theoretical results in (30) perfectly match the simulation results, indicating the significant accuracy of our analysis. In Fig. 3, we also plot the simulation results of DL/UL SINRs for $B = 14$ and it is shown that the removal of distant small cells from our analysis has a small impact on the SINR performances because the difference between the results of $B = 12$ and those of $B = 14$ is marginal, especially in the practical SINR region of $[-20, 40]$ dB, indicating diminishing return of including more small cells into the analysis.

### *C. The Proposed Partial IC Scheme*

From Fig. 3, we can draw two basic conclusions as follows:

- Dynamic TDD is beneficial to the DL because the UL-to-DL interference in the dynamic TDD DL is generally weaker than the DL-to-DL one in the static TDD DL.
- The DL-to-UL interference in the dynamic TDD UL needs to be suppressed, otherwise UEs may have an average outage probability (OP) of about 8 % for the event that $Z_1^{\mathrm{UL}} \leq$ -5 dB.

It is also important to note that the tail of the dynamic TDD UL SINR CDF curve in Fig. 3 should not be interpreted as only cell-edge UEs suffering from heavy DL-to-UL interference. In fact, cell-center UEs are also vulnerable to dominant DL-to-UL interference in dynamic TDD. This is because BS-to-BS path loss could be orders of magnitude smaller than the BS-to-UE path loss, as indicated earlier, and because the UL interference does not depend on the UE position but on that of the serving BS, which is fixed. In order to illustrate this, we relocate UE $K_1$ inward with $d_{11} = 0.01$ km and plot the UL SINR CDFs for dynamic TDD in Fig. 4. As can be seen from Fig. 4, the heavy tail of the dynamic TDD UL SINR still exists, which indicates undesirable outage behavior, even for cell-center UEs, when the DL-to-UL interference is overwhelming. Thus, interference mitigation for dynamic TDD should consider both cell-edge and cell-center UEs.

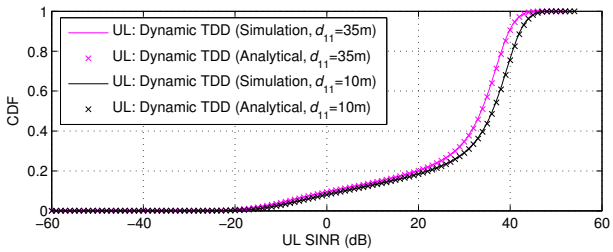


Fig. 4. CDFs of the UL SINRs for different UEs with dynamic TDD.

In order to combat the DL-to-UL interference, we proposed in [4] that interference cancellation (IC) techniques should be considered. However, full IC, i.e., cancelling DL interference from all $B - 1$ small cells would impose very high burdens on the network side and thus may cause a number of implementation issues such as complex signal processing operations at BSs and excessive information exchange of DL transmission assumptions in the small cell backhaul. Here, we propose a partial IC scheme, in which only strong DL-to-UL interference shall be cancelled. To be more specific, we propose that the interference from small cell $b$ is cancelled only if its large-scale attenuation, i.e., $\left(PL_b^{\mathrm{BS2BS}} + S_b^{\mathrm{BS2BS}}\right)$, is smaller than $\delta$. Note that $\delta = \infty$ and $\delta = 0$ correspond to the full IC case and the non-IC case, respectively. To emulate the IC operation, for an interference-cancelled (ICed) small cell with DL transmissions, its index will be transferred from $\Psi^{\mathrm{DL}}$ to $\Psi^{\mathrm{M}}$ in (30). For a particular $\delta$, the average OP for the event that, e.g., $Z_1^{\mathrm{UL}} < \xi$, can be obtained by averaging $P_{Z_1}(\xi)$ in (30) over all drops. Through a standard bisection search process [9], we can find the appropriate $\delta$ that keeps the average OP below a threshold $\kappa^{\mathrm{OP}}$. The bisection search process is terminated when the target OP is achieved within a gap of $\epsilon$. In our example, we first focus on low traffic loads $\rho_0 = 0.3$, and choose $\xi =$ -5 dB, $\kappa^{\mathrm{OP}} = 0.01$ and $\epsilon = 0.001$. The initial values of $\delta$ are respectively set to 50 dB and 90 dB, where the corresponding OPs create a sufficiently large interval containing $\kappa^{\mathrm{OP}}$. The results of the bisection search process is tabulated in Table II, including the values of $\delta$, average OPs, and average numbers of ICed cells. As can be seen from Table II, $\delta =$ 85 dB satisfies the requirements and the average number of ICed cells for UE $K_1$ is only 0.48, showing a much lower complexity of the proposed partial IC scheme compared with the full IC scheme. The proposed bisection search is also conducted for a medium traffic load case with $\rho_0 = 0.5$, which results are presented in Table III. From Table III, we can observe that $\delta =$ 87.5 dB and the average number of ICed cells is still less than one.

$$
\begin{aligned}
P_Z(z) &= \Pr\left(\tfrac{\beta X}{Y^{\mathrm{sum}}+1} \le z\right) \\
&= \int_0^{+\infty} P_X\left(\tfrac{z(y+1)}{\beta}\right) p_{Y^{\mathrm{sum}}}(y)\, dy \\
&\approx \int_0^{+\infty} \left\{1 - \exp\left(-\tfrac{z(y+1)}{\beta}\right) \sum_{l=0}^{N-1} \tfrac{1}{l!}\left[\tfrac{z(y+1)}{\beta}\right]^l\right\} \tfrac{\omega^\lambda}{\Gamma(\lambda)} \exp(-\omega y)\, y^{\lambda-1} dy \\
&= \int_0^{+\infty} \tfrac{\omega^\lambda}{\Gamma(\lambda)} \exp(-\omega y)\, y^{\lambda-1} dy - \int_0^{+\infty} \left\{\exp\left(-\tfrac{z+zy}{\beta}\right) \sum_{l=0}^{N-1} \tfrac{1}{l!}\left(\tfrac{z}{\beta} + \tfrac{z}{\beta} y\right)^l\right\} \tfrac{\omega^\lambda}{\Gamma(\lambda)} \exp(-\omega y)\, y^{\lambda-1} dy \\
&= 1 - \tfrac{\omega^\lambda}{\Gamma(\lambda)} \exp\left(-\tfrac{z}{\beta}\right) \int_0^{+\infty} \left\{\exp\left(-\tfrac{z+\omega\beta}{\beta} y\right) \sum_{l=0}^{N-1} \tfrac{1}{l!}\left(\tfrac{z}{\beta}\right)^l \sum_{k=0}^{l} \mathrm{C}_l^k y^k y^{\lambda-1}\right\} dy \\
&= 1 - \tfrac{\omega^\lambda}{\Gamma(\lambda)} \exp\left(-\tfrac{z}{\beta}\right) \sum_{l=0}^{N-1} \sum_{k=0}^{l} \tfrac{1}{k!(l-k)!}\left(\tfrac{z}{\beta}\right)^l \int_0^{+\infty} \exp\left(-\tfrac{z+\omega\beta}{\beta} y\right) y^{k+\lambda-1} dy \\
&= 1 - \tfrac{\omega^\lambda}{\Gamma(\lambda)} \exp\left(-\tfrac{z}{\beta}\right) \sum_{l=0}^{N-1} \sum_{k=0}^{l} \tfrac{\Gamma(k+\lambda)\left(\frac{z}{\beta}\right)^l}{k!(l-k)!}\left(\tfrac{z+\omega\beta}{\beta}\right)^{-(k+\lambda)} \int_0^{+\infty} \tfrac{\left(\frac{z+\omega\beta}{\beta}\right)^{k+\lambda}}{\Gamma(k+\lambda)} \exp\left(-\tfrac{z+\omega\beta}{\beta} y\right) y^{k+\lambda-1} dy \\
&= 1 - \tfrac{\omega^\lambda}{\Gamma(\lambda)} \exp\left(-\tfrac{z}{\beta}\right) \sum_{l=0}^{N-1} \sum_{k=0}^{l} \tfrac{\Gamma(k+\lambda)}{k!(l-k)!}\left(\tfrac{z}{\beta}\right)^l \left(\tfrac{\beta}{z+\omega\beta}\right)^{k+\lambda} \\
&\triangleq Q(\omega, \lambda, \beta, z). \qquad (32)
\end{aligned}
$$

Table II
BISECTION SEARCH OF $\delta$ ($\rho_0 = 0.3$)

| Search No. | $\delta$ (dB) | Average OP | Average # of ICed cells |
|---|---|---|---|
| 1 | 50 | 0.0678 | 0 |
| 2 | 90 | 0.0052 | 0.66 |
| 3 | 70 | 0.0645 | 0.02 |
| 4 | 80 | 0.0252 | 0.30 |
| 5 | 85 | 0.0100 | 0.48 |

Table III
BISECTION SEARCH OF $\delta$ ($\rho_0 = 0.5$)

| Search No. | $\delta$ (dB) | Average OP | Average # of ICed cells |
|---|---|---|---|
| 1 | 50 | 0.1100 | 0 |
| 2 | 90 | 0.0087 | 0.66 |
| 3 | 70 | 0.1058 | 0.02 |
| 4 | 80 | 0.0421 | 0.30 |
| 5 | 85 | 0.0167 | 0.48 |
| 6 | 87.5 | 0.0107 | 0.59 |

## V. CONCLUSION

This work sheds new light on the fundamentals of dynamic TDD transmissions by presenting for the first time a theoretical analysis on the SINR performance of dynamic TDD in homogeneous small cell networks. Based on such framework, a partial IC scheme is proposed to accurately control the DL-to-UL interference using closed-form computations as well as a standard bisection search, so that the average OP for a given SINR can be kept under a required threshold in the UL. It is shown that cancelling one interfering small cell on average is good enough when the traffic load is low to medium to avoid radio link failures.

## APPENDIX I: PROOF OF LEMMA 1

We rewrite $\mathbf{H}_b^{\mathrm{BS2BS}}$ as $\left[\mathbf{h}_{b,(1)}^{\mathrm{BS2BS}}, \ldots, \mathbf{h}_{b,(n)}^{\mathrm{BS2BS}}, \ldots, \mathbf{h}_{b,(N)}^{\mathrm{BS2BS}}\right]^{\mathrm{T}}$, where $\mathbf{h}_{b,(n)}^{\mathrm{BS2BS}}$ is the channel vector from the BS of cell $C_b$ to the $n$-th antenna of the BS of cell $C_1$. Then, for a given $\mathbf{w}_b$, $\mathbf{h}_{b,(n)}^{\mathrm{BS2BS}}\mathbf{w}_b$ can be regarded as a weighted sum of $N$ i.i.d. Rayleigh fading coefficients, which leads to a new Rayleigh fading coefficient, since the norm of $\mathbf{w}_b$ is one and the phases of the elements in $\mathbf{h}_{b,(n)}^{\mathrm{BS2BS}}$ and $\mathbf{w}_b$ are random and uncorrelated. Thus, $\mathbf{H}_b^{\mathrm{BS2BS}}\mathbf{w}_b$ becomes a column vector with its entries being i.i.d. Rayleigh fading coefficients. Similarly, for a given $\mathbf{f}_1$, $\mathbf{f}_1\mathbf{H}_b^{\mathrm{BS2BS}}\mathbf{w}_b$ can be regarded as a weighted sum of $N$ i.i.d. Rayleigh fading coefficients, which yields another new Rayleigh fading coefficient. Therefore, the squared norm of $\mathbf{f}_1\mathbf{H}_b^{\mathrm{BS2BS}}\mathbf{w}_b$ is a chi-squared RV with 2 degrees of freedom, which concludes our proof.

## APPENDIX II: PROOF OF THEOREM 2

From (20), (21) and (23), the CDF of $Z$ can be derived in (32), which concludes our proof.

## REFERENCES


[1] 3GPP, "TR 36.828 (V11.0.0): Further enhancements to LTE Time Division Duplex (TDD) for Downlink-Uplink (DL-UL) interference management and traffic adaptation," Jun. 2012.

[2] 3GPP, "TS 36.213 (V11.2.0): Physical layer procedures," Feb. 2013.

[3] Z. Shen, A. Khoryaev, E. Eriksson, X. Pan, "Dynamic uplink-downlink configuration and interference management in TD-LTE," IEEE Communications Magazine, vol. 50, no., 11, pp. 51-59, Nov. 2012.

[4] M. Ding, D. López Pérez, A. V. Vasilakos, and W. Chen, "Dynamic TDD transmissions in homogeneous small cell networks," *IEEE International Conference on Communications (ICC) 2014*, pp.1-6, June 2014.

[5] J. Proakis, Digital Communications (Third Ed.), McGraw-Hill, 1995.

[6] A. H. Feiveson and F. C. Delaney, "The distribution and properties of a weighted sum of Chi squares," NASA's technical note, TN D-4575, May 1968.

[7] ETSI MCC, "Draft Report of 3GPP TSG RAN WG1 #75," Nov. 2013.

[8] P. Skillermark, M. Almgren, D. Astely, M. Lundevall and M. Olsson, "Simplified Interference Modeling in Multi-Cell Multi-Antenna Radio Network Simulations," *IEEE Vehicular Technology Conference (VTC) Spring 2008*, pp.1886-1890, May 2008.

[9] R. L. Burden and J. D. Faires, Numerical Analysis (Third Ed.), PWS Publishers, 1985.